water

MDPI

Article

Stream Network Modeling Using Remote Sensing Data in an Alpine Cold Catchment

Hong Cao [1,2,3], Zhao Pan [3], Qixin Chang [4], Aiguo Zhou [3], Xu Wang [5,*] and Ziyong Sun [3]

1 Hubei Key Laboratory of Intelligent Geo-Information Processing, China University of Geosciences, Wuhan 430074, China; ghg_ch@126.com
2 School of Computer Sciences, China University of Geosciences, Wuhan 430074, China
3 School of Environmental Studies, China University of Geosciences, Wuhan 430074, China; panzhao@cug.edu.cn (Z.P.); aiguo.zhou@cug.edu.cn (A.Z.); ziyong.sun@cug.edu.cn (Z.S.)
4 College of Environment and Civil Engineering, Chengdu University of Technology, Chengdu 610059, China; changqixin@hotmail.com
5 School of Geography and Information Engineering, China University of Geosciences, Wuhan 430074, China
* Correspondence: wangxu@cug.edu.cn

Abstract: The hydrological information derived from a digital elevation model is very important in distributed hydrological modeling. As part of alpine hydrological research on stream network modeling using remote sensing data in the northeast of the Tibetan Plateau, three digital elevation model (DEM) datasets were obtained for the purpose of hydrological features, mainly including channel network, watershed extent and terrain character. The data sources include the airborne light detection and ranging (LiDAR) with point spacing of 1 m, the High Mountain Asia (HMA) DEM and the Shuttle Radar Topography Mission (SRTM) DEM. Mapping of the watershed and stream network was conducted using each of the three DEM datasets. The modeled stream networks using the different DEMs were verified against the actual network mapped in the field. The results show that the stream network derived from the LiDAR DEM was the most accurate representation of the network mapped in the field. The SRTM DEM overestimated the basin hypsometry relative to the LiDAR watershed at the lowest elevation, while the HMA DEM underestimated the basin hypsometry relative to the LiDAR watershed at the highest elevation. This may be because, compared with the SRTM DEM and the HMA DEM, the LiDAR DEM has higher initial point density, accuracy and resolution. It can be seen that the LiDAR data have great potential for the application in hydrologic modeling and water resource management in small alpine catchments.

Keywords: hydrological modeling; LiDAR; stream network

Citation: Cao, H.; Pan, Z.; Chang, Q.; Zhou, A.; Wang, X.; Sun, Z. Stream Network Modeling Using Remote Sensing Data in an Alpine Cold Catchment. *Water* **2021**, *13*, 1585. https://doi.org/10.3390/w13111585

Academic Editors: Gui Jin, Qian Zhang and Feng Wu

Received: 17 April 2021
Accepted: 27 May 2021
Published: 4 June 2021

1. Introduction

The hydrological characteristic information of stream networks has an important application value in water resources management, land management, forestry management, groundwater monitoring and other natural resources management [1–6]. The hydrological parameters are also important components when modeling the hydrologic response of a watershed to a precipitation event, especially for the distributed watershed hydrological modeling, as well as for the modeled runoff lag time influenced by the hillslope travel distance and stream network link lengths [7]. Even in some ungauged areas, the flow indices extracted from the digital elevation model can be used as an input to the hydrological models [8]. Accurate description of spatial hydrologic information such as a stream network is also a precondition for the effective distributed catchment modeling [9,10]. The geographic information system (GIS) modeling method, which uses the digital elevation model (DEM) to extract watershed attributions such as channel network, watershed extent and terrain character is a common method for the runoff simulation.

Compared with the traditional method of identifying stream networks from aerial photographs, the flow accumulation algorithm based on GIS is more efficient in delineating

stream networks [11–13]. With the growing availability of high–resolution stereo images and the use of different flow accumulation algorithms [14–16], there have been plenty of studies using DEM extracted from remote sensing data to delineate more detailed hydrological information, including flow direction, accumulation of confluence, flow length and stream network, etc. [17–20]. These studies have effectively demonstrated that stream network modeling has positive significance for the analysis of watershed hydrological and geomorphic characteristics, but there is a lack of comparison and analysis of a variety of DEM data for the stream network modeling. LiDAR can be used to create DEM better than the conventional DEM derived from the traditional photogrammetric method or from topographic maps in terms of resolution and accuracy [21,22]. The accuracy of DEM extracted from the LiDAR data as well as hydrological features related to surface topography has a significant potential for improving hydrologic modeling [23,24]. Although LiDAR has certain advantages in accuracy, it also has some limitations in acquisition difficulty and cost. As free datasets, the SRTM DEM and the HMA DEM are easier to obtain.

Due to the complicated terrain and special climate in the alpine, the water resources problem has been paid more and more attention by the government and society. Therefore, the way to effectively obtain the stream network data in an alpine region and then effectively manage the local water resources is particularly critical. In this study, the SRTM DEM, the HMA DEM and the LiDAR data were used to model stream networks in a small alpine cold catchment with field–mapped stream channels. The compared stream networks included the field–mapped channels, networks modeled using the SRTM DEM, high–resolution stereo imagery DEM and the LiDAR DEM, respectively. Furthermore, the hydrological characteristics derived from these three DEMs were compared with the topographic features, watershed and elevation information.

2. Study Area, Data and Methods

2.1. Study Area

The Hongnigou (HNG) Basin is a small alpine cold catchment in the Qilian mountains of the Heihe Basin, China (38°21′14″ N, 99°52′30″ E). It is located in the northeast of the Tibetan Plateau. The small catchment is located on the eastern slope of the Hulugou Basin and flows into the Heihe River (Figure 1).

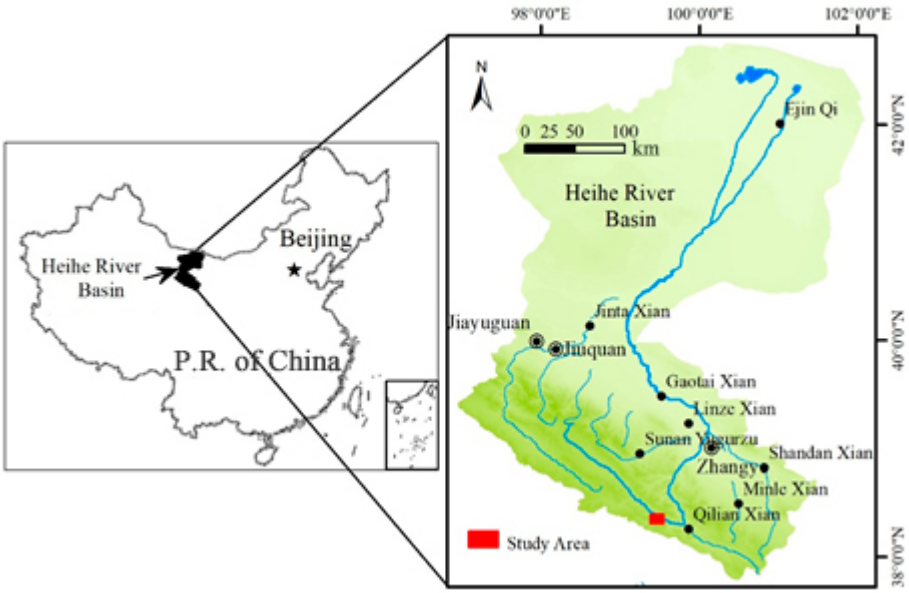

Figure 1. Location of the study area.

The topography of the watershed area is gently sloped. The upper part of the basin is covered with stone, fine sand, silt, shrubs and grasslands. The surface of the lower layer is

fine sand, silt and clay deposits, mainly covering alpine meadows. The ground is covered with alpine meadows. In the middle of the watershed area, the surface of the terrain is cut 1~2 m by the stream network. The climate in the area is continental, with an average temperature of 1–2 °C and annual precipitation of 600 mm. The stream network disruption occurs from November to March next year. The area is characterized by alpine grasslands, marshlands and steppes.

2.2. Field Mapping of the Stream Network

Field surveys were carried out along the streams. All the streams were walked up to the steep slopes or the flat ground where the channels terminated with poor drain (Figure 2a). The streams were delineated by tracing the streams on the Quickbird image and recording regular global positioning system (GPS) sites. The GPS device was placed close to the surface of the earth when recording the track of the stream channel. The elevation of GPS points can be considered as the actual elevation of the land surface. Field survey and monitoring have shown that stream disruption usually occurs between November and March next year. There are also dried channels caused by changeable stream channels, which make the land surface ragged (Figure 2b).

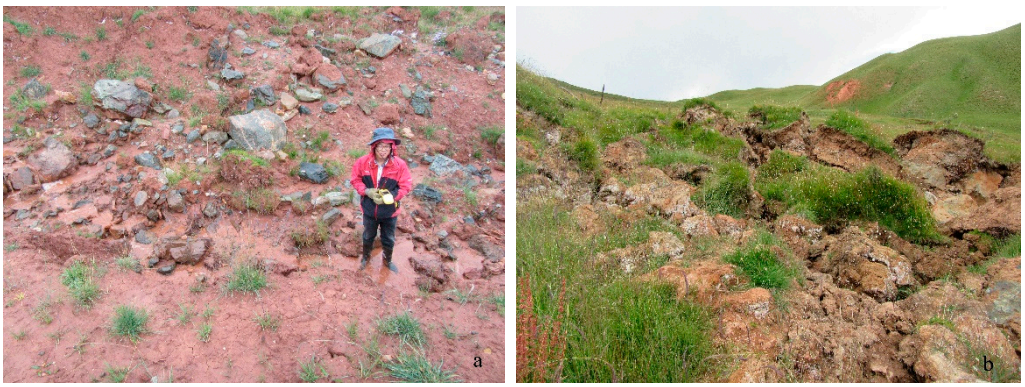

Figure 2. Photos taken at the field work. (**a**) Field work about the drainage network survey on July 06, 2015, and (**b**) the ragged land surface in the HNG catchment.

2.3. Digital Elevation Model Sources

During the 11 days of the SRTM mission in February 2000, the SRTM mapped the surface of the Earth numerous times from different perspectives by using imaging radar. The SRTM data were acquired by using a C–band radar and an additional antenna. In late 2015, the 30-m, 1-arcsecond terrain data generated by the NASA'S SRTM was released globally. The SRTM data used in this study were downloaded from the USGS [25].

The High Mountain Asia (HMA) 8–m digital elevation model (DEMs) data were downloaded from the NASA National Snow and Ice Data Center Distributed Active Archive Center (NSIDC DAAC). The ground resolution of the nadir image is 0.5 m. The DEM was generated using Worldview–2 ultra-high–resolution along–track stereo pairs acquired on 30 March 2016.

The LiDAR data were obtained using a Leica ALS70 (Leica Geosystems AG Heerbrugg, Switzerland) carried on a Harbin Y–12 plane (Harbin Aircraft Industry Group, Harbin, China) flying at an average altitude of 4800 m on 25 July 2012. The flying speed was 220 km/h with the scan angle of 23°. The point density was specified as an average of 1 point/m^2. The LiDAR elevation points were received with a resolution of 1 m and processed as a DEM, with an estimated vertical accuracy of about 0.5 m in flat areas.

Considering that the objective of this study was to compare hydrological features extracted from different DEM data sources, these DEM data were projected to the same projection system. All these data were re–projected in the WGS_1984_UTM_Zone_47N reference frame, with elevation referred to the D_WGS_1984 ellipsoid. In order to facilitate

the comparison of subsequent hydrological extraction from DEM data, ArcGIS 10.2 was used to resample the DEM dataset with a resolution of 10 m.

The elevation values collected at 214 GPS points in the HNG basin during field work were used to verify the precision of the DEM derived from the SRTM DEM, stereo imagery and the LiDAR data.

2.4. Modeling Stream Networks Using DEMs

The stream networks were modeled by using the hydrological analysis module of ArcGIS. In order to ensure that flow was not changed by artificial depressions, the filling function was used in producing a DEM without depressions. The flow direction based on a deterministic eight–node algorithm (D8) is simple, increasing efficiency numerically [26]. It was then used to generate the flow directions grids which were applied to create the surface flow accumulation network to initiate the stream flow network. To verify the accuracy of the modeled stream network by using the DEM, the buffer zone was created by the mapped stream network in the field within a 10 m buffer.

3. Results and Discussion

3.1. Field–Mapped Stream Networks Assisted with High–Resolution Images

In the preliminary work of the study, we used high–resolution images to assist the field survey of the stream network. Figure 3 shows the surveyed stream channel network in field work and the interpreted channel stream by using a high–resolution image. GPS points measured in the field along the stream represent a similar stream net pattern to that mapped in the high–resolution image. However, many small stream curves are missed in the process of GPS point acquisition. High–resolution remote sensing images have rich spatial texture information, which is helpful to interpret the small channels. Therefore, stream details can be interpreted using high–resolution images.

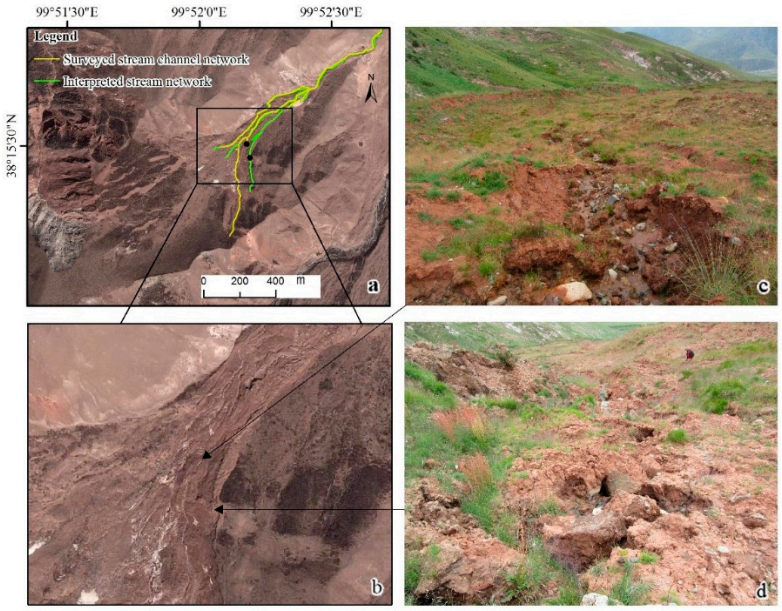

Figure 3. The surveyed stream channel network in field work and interpreted channel stream by using the high-resolution image. (**a**) shows the field-mapped stream networks with the aids of GPS and high-resolution image. (**b**) reflects the location of photos c and d. (**c**) is a photo of stream during tracking along the stream, and (**d**) is a photograph captured for the dried ditch.

The photos in Figure 3c,d were taken during the field work in July 2015. It is clear that the land surface is now rugged, which was once a stunning mountain meadow, and the criss–cross ditches connect to the stream, which makes it difficult to determine the drainage network. Stream disruption occurs from November to March next year. Furthermore, small

and ephemeral flow streams are difficult to identify in the high–resolution image, especially when channels are hidden under the vegetation. This also means that there may be some deviation in the discrimination of the high–resolution image. It is noticeable that there are inaccuracies in the interpreted stream location in reference to field–mapped channels, such as the stream channel can be offset by up to 10 m.

Therefore, the interpreted stream network was corrected with the aid of GPS and a digital camera. The total channel length was 2546 m. Although there are some differences in the stream network interpreted by the high–resolution image, we also found some dry stream channels. This may be the result of no surface water or underground water recharge after the processes of frozen soil thawing. The subsidence of the land surface changed the landform and destroyed the grassland, and the change of landform had a great influence on the stream network.

In addition, we believe that some of the differences between the two stream networks may be caused by the time difference. The high–resolution image was received in March 2013. However, the drainage channel was surveyed in July 2015. The field work of tracking the stream channel is required to obtain a true drainage network by using a high–resolution image.

3.2. Stream Networks Modeled Using DEM Derived from SRTM, HMA and LiDAR Data

Figure 4 shows the stream channel network and watershed boundary modeled by the SRTM DEM, HMA stereo pair images and the LiDAR data. The difference in resolution can be clearly seen by shading the relief images. The three types of DEM show the similar terrain surface generally. However, the LiDAR DEM reflects more terrain details than the SRTM DEM and the HMA DEM because of higher spatial resolution.

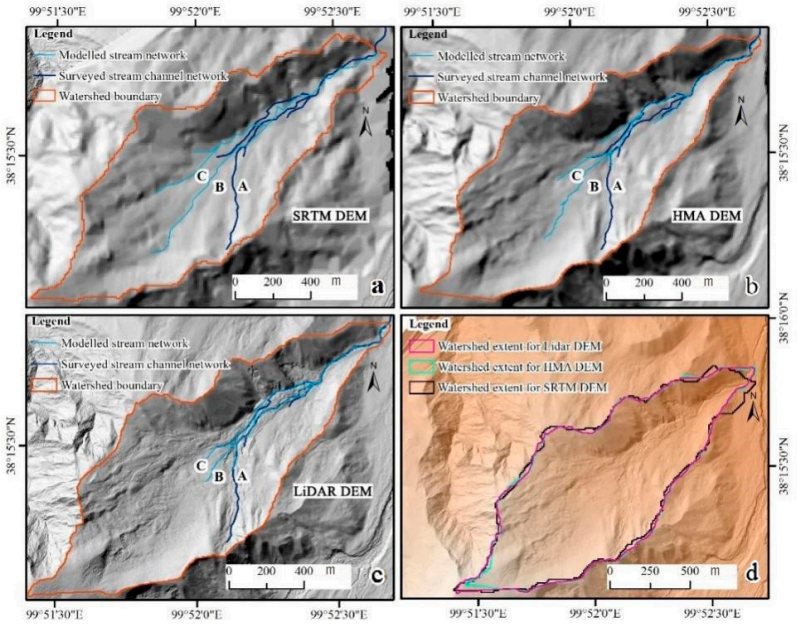

Figure 4. Stream network and watershed boundary modeled using (**a**) the SRTM DEM resampled with a resolution of 10 m, (**b**) 8 m HMA DEM derived from a high–resolution stereo pair image, (**c**) the LiDAR DEM with a resolution of 1 m, (**d**) watershed extents for the LiDAR DEM (red), HMA DEM, interpolated SRTM DEM of 10 m (black).

As for the lower elevation zone of the catchment, the stream networks modeled by the DEM of SRTM, HMA and the LiDAR are generally similar (Figure 4). However, there are some noticeable differences. Compared with the HMA DEM and the SRTM DEM, the data extracted from the LiDAR data have more complex topographic surface and better consistency with field–mapped channels. By comparing with the actual survey results,

stream networks extracted from the SRTM DEM have unnaturally angular characteristics and line segments. This may be caused by the lower spatial resolution and the point density of the SRTM DEM obtained by a shuttle radar. Therefore, fine terrain features derived from this resolution, such as confluence of streams and small channels, are absent.

Compared with the stream channels extracted by the LiDAR DEM, those extracted from the SRTM DEM extend further upslope. The channel length modeled by the LiDAR DEM is 2964 m, while that modeled by the SRTM DEM is 2643 m (Table 1). Due to the improved capture of the terrain detail of channel curves and stream confluents, the channels derived from the LiDAR DEM matched much better to the channel mapping of field work survey than the HMA DEM and the SRTM DEM. For the channel A, it cannot be modeled by the SRTM DEM with low spatial resolution. However, it can only be modeled partly by using the HMA DEM and the LiDAR DEM. This may be a result of the criss–cross crevices on the topographic surface caused by thawing frozen soil. In addition, there exists a small–scale landslide in the upper part of channel A.

Table 1. Summary of stream networks derived from different sources.

	LiDAR DEM	HMA DEM	SRTM DEM	Field Survey
Network length (m)	2964	2712	2643	2546
Accuracy (%)	76.08	43.26	10.02	100

It can also be observed that channels B and C modeled by the three DEMs extended upslope further than those mapped in the field with the high–resolution image. The entire channel length modeled using the LiDAR DEM and the HMA DEM was nearly 1.2 and 1.5 times as long as that of the surveyed channels in the field (Table 1). It was clear that modeled channels from the LiDAR DEM have the highest accuracy. The LiDAR survey, with a greater point density, capture the detailed land surface of this small watershed area at a higher resolution. This explains why high-resolution DEM models stream network and watershed better than the SRTM DEM, especially in a small watershed [24]. Pirotti (2010) indicated that LiDAR point density used to interpolate the 1 m DEM to extract the channel network can be as low as 1 point per 5 m^2 [27]. In a small alpine catchment, however, DEM can accurately reflect the land surface. The smaller the basin area is, the more obvious the impact of geomorphic attribute differences on the hydrological model is [28].

The field–mapped stream network is composed of channels with water flow. However, the upstream of the modeled network is relative to the flat area of swamp, where there are dozens of small ponds. It should be noted that the stream network in the alpine watershed may change due to the land surface mostly affected by the freezing and thawing process of frozen soil. Seasonal frozen soils degradation may cause changes in land characteristics and drainage system.

3.3. Watershed Delineation Using LiDAR DEM, HMA DEM and SRTM DEM

The coverage area of watersheds derived from the DEMs is showed in Table 2. The delineation for the watershed of Hongni Gou is similar (Figure 4d). The area of the SRTM DEM in the basin is different from that of the other two kinds of DEM with higher resolution in the different elevation range (Table 2).

Table 2. Overall elevation statistics for each derived watershed.

Statistics	LiDAR DEM	HMA DEM	SRTM DEM
Area (ha)	112.3	111.2	112.47
Min elevation (m)	2996	2995.83	3052
Max elevation (m)	3589	3582.08	3623
Mean elevation (m)	3276.39	3274.73	3315
Elevation range (m)	593	587	571

The Hongni Gou watershed area was 112.3 ha with elevations from 2996 m to 3589 m as determined by using the LiDAR DEM. The area of the watershed created using the HMA DEM was within 1.1 ha (or 1%) smaller than the baseline LiDAR–determined watershed, while the watershed created from the SRTM DEM was 0.17 ha (or 0.15%) larger than the baseline LiDAR watershed. It looks like the watershed derived from the SRTM DEM was more accurate than the DEM generated from high–resolution images from Digital Globe Inc. However, it is clear from Figure 4d that for the SRTM DEM, the differences in the generated watershed boundaries were mainly near the watershed outlet.

Results for the HMA DEM show a similar pattern besides a watershed difference that occurred at the upper reaches on the southwestern side. The extent of the watershed between the LiDAR data and stereo pairs data has a reduced difference, although the difference in the area of the watershed is larger than with the SRTM DEM. It indicates that the terrain information near the basin outlet contained within both the SRTM DEM and the HMA DEM was different from the LiDAR DEM, while at the edges of the watershed boundaries of the upper streams, the terrain information contained within both the HMA DEM and the LiDAR DEM was significantly different from the SRTM DEM. That may be caused by the different sampling method. Relative to high resolution–based methods, the LiDAR data are better at receiving signal at shadow areas while sampling at the side of sharp ridges [29].

The DEM can reflect the surface land features that affect the modeling of surface channels by blocking and channeling them. Figure 5 shows that the elevation of the SRTM DEM is higher than in the LiDAR DEM and the HMA DEM. As for the elevation, the difference of the average elevation of the LiDAR DEM and the HMA DEM is less than 2 m, while the elevations derived from the SRTM DEM are generally larger. The watershed hypsometry illustrated a greater area at the higher altitudes from 3300 m to 3640 m and a smaller area at the lower altitudes from 3000 m to 3300 m. It is consistent with the data in Table 2. It suggested that the HMA DEM and LiDAR hypsometry is similar in this height range. In general, the LiDAR DEM data are more conducive to the simulation of stream network modeling in an alpine cold catchment if conditions permit. At the same time, the HMA DEM is a good substitute for the LiDAR DEM. The advantage of the SRTM DEM lies in the division of the watershed.

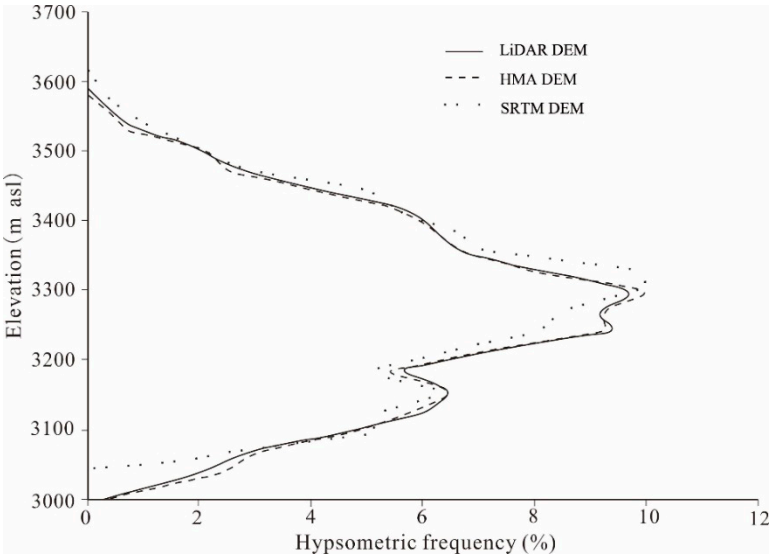

Figure 5. Watershed hypsometry for the DEM extracted from the LiDAR DEM, high–resolution stereo pairs and the SRTM DEM.

It should be noted that we further compared the differences between the three kinds of DEM by counting eight geomorphological parameters, such as mean slope, mean aspect,

mean topographic relief, mean surface roughness, mean slope of the slope, mean slope of the aspect, mean incision depth and maximum curvature, as shown in Table 3. Through the comparative analysis, it can be seen that the LiDAR DEM has obvious differences in the description of the terrain in the study area compared with the other two kinds of DEM, but the HMA DEM is closer to it. The SRTM DEM has undergone interpolation resampling, but its description of the landform is relatively rough.

Table 3. Geomorphic characteristic parameters of three kinds of DEM.

Characteristic	LiDAR DEM	HMA DEM	SRTM DEM
Mean slope	20.9018	19.3394	19.1592
Mean aspect	113.9193	112.4902	96.6869
Mean topographic relief	1.0064	7.1110	8.6557
Mean surface roughness	1.0849	1.0689	1.0692
Mean slope of the Slope	54.0766	19.3394	13.0540
Mean slope of the Aspect	75.8926	44.1983	40.9861
Mean incision depth	0.5032	3.5452	4.3246
Maximum curvature	1180.5176	15.7341	13.7034

Further, we compare the three DEMs with the elevation data onto the GPS points measured (Figure 6). It can be seen that the LiDAR DEM and the HMA DEM are basically consistent with the measured data, and the error between the SRTM DEM and the measured data is large. The standard deviation from elevation values in the HNG catchment of the SRTM DEM, stereo imagery and the LiDAR DEM was 5.46 m, 3.75 m and 1.41 m.

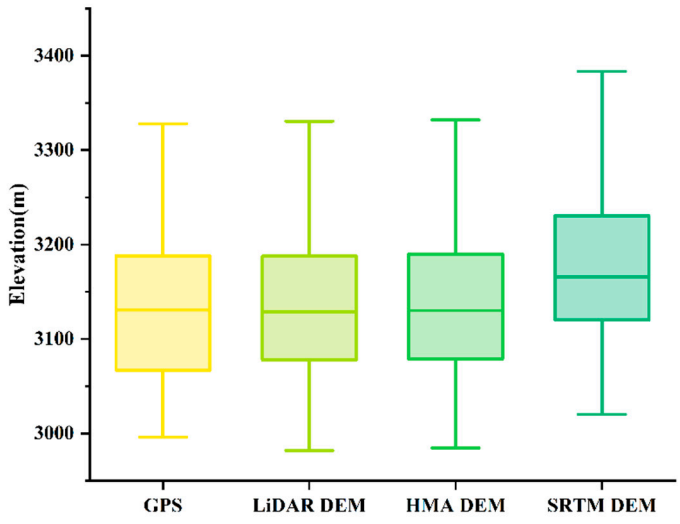

Figure 6. Difference between three kinds of DEM and GPS data.

4. Conclusion

DEMs capture the surface topography features, which is the basis for the deriving hydrological information related to terrain, such as stream network, watershed boundary, etc. This paper focused on investigating different DEMs for hydrological attributes in a small alpine cold catchment. The quality and resolution of DEM data constantly increased from the SRTM DEM to the HMA DEM to the LiDAR DEM. The stream network modeled from the LiDAR DEM was consistent with the actual field–mapped network mostly, and it was even more precise than that interpreted by the high–resolution imagery. Differences in catchment attributes because of different DEM sources could impact hydrological parameter and runoff predictions during distributed hydrological modeling processes. Furthermore, the denser the point cloud of the LiDAR for producing DEMs, the more detailed is the complex land surface for hydrological parameters, which were the basis of constructing the distribution hydrological model. The LiDAR DEM is useful to improve

hydrologic features of modeling and management. This research has possible implications for the stream flow modeling in alpine cold areas.

Author Contributions: Conceptualization, H.C. and X.W.; methodology, H.C.; validation, Z.P. and Q.C.; formal analysis, H.C.; investigation, Z.P. and Q.C.; resources, A.Z.; data curation, H.C.; writing—original draft preparation, H.C.; writing—review and editing, X.W.; project administration, X.W. and Z.S.; funding acquisition, X.W. and Z.S. All authors have read and agreed to the published version of the manuscript.

Funding: This research was funded by the National Natural Science Foundation of China (grant Nos. 41401076, 91125009) and the China University of Geosciences (grant No. CUG160818).

Institutional Review Board Statement: Not applicable.

Informed Consent Statement: Not applicable.

Data Availability Statement: Not applicable.

Acknowledgments: The authors thank the Northwest Institute of Eco–Environment and Resources (CAS) for providing LiDAR data for this study.

Conflicts of Interest: The authors declare no conflict of interest.

References

1. Knouft, J.H.; Botero-Acosta, A.; Wu, C.-L.; Charry, B.; Chu, M.L.; Dell, A.I.; Hall, D.M.; Herrington, S.J. Forested Riparian Buffers as Climate Adaptation Tools for Management of Riverine Flow and Thermal Regimes: A Case Study in the Meramec River Basin. *Sustainability* **2021**, *13*, 1877. [CrossRef]
2. Sun, Z.; Ma, R.; Wang, Y.; Hu, Y.; Sun, L. Hydrogeological and hydrogeochemical control of groundwater salinity in an arid inland basin: Dunhuang Basin, northwestern China. *Hydrol. Process.* **2016**, *30*, 1884–1902. [CrossRef]
3. Van Loon, A.F.; Laaha, G. Hydrological drought severity explained by climate and catchment characteristics. *J. Hydrol.* **2015**, *526*, 3–14. [CrossRef]
4. Lee, J.Y.; Yi, M.J.; Hwang, D. Dependency of hydrologic responses and recharge estimates on water-level monitoring locations within a small catchment. *Geosci. J.* **2005**, *9*, 277–286. [CrossRef]
5. Jin, G.; Chen K., L.; Wang, P.; Guo B., S.; Dong, Y.; Yang, J. Trade-offs in land-use competition and sustainable land development in the North China Plain. *Technol. Forecast Soc. Chang.* **2019**, *141*, 36–46. [CrossRef]
6. Jin, G.; Shi, X.; He D., W.; Guo B., S.; Li Z., H.; Shi X., B. Designing a spatial pattern to rebalance the orientation of development and protection in Wuhan. *J. Geogr. Sci.* **2020**, *30*, 569–582. [CrossRef]
7. Li, J.; Zhao, Y.; Bates, P.; Neal, J.; Tooth, S.; Hawker, L.; Maffei, C. Digital Elevation Models for topographic characterisation and flood flow modelling along low-gradient, terminal dryland rivers: A comparison of spaceborne datasets for the Río Colorado, Bolivia. *J. Hydrol.* **2020**, *591*, 125617. [CrossRef]
8. Althoff, D.; Ribeiro, R.B.; Rodrigues, L.N. Gauging the Ungauged: Regionalization of Flow Indices at Grid Level. *J. Hydrol. Eng.* **2021**, *26*, 04021008. [CrossRef]
9. Godsey, S.E.; Kirchner, J.W. Dynamic, discontinuous stream networks: Hydrologically driven variations in active drainage density, flowing channels and stream order. *Hydrol. Process.* **2014**, *28*, 5791–5803. [CrossRef]
10. Clarke, S.; Burnett, K. Comparison of Digital Elevation Models for Aquatic Data Development. *Photogramm. Eng. Remote. Sens.* **2003**, *69*, 1367–1375. [CrossRef]
11. Roux, C.; Alber, A.; Bertrand, M.; Vaudor, L.; Piégay, H. "FluvialCorridor": A new ArcGIS toolbox package for multiscale riverscape exploration. *Geomorphology* **2015**, *242*, 29–37. [CrossRef]
12. Sen, A.; Gokgoz, T. An experimental approach for selection/elimination in stream network generalization using support vector machines. *Geocarto Int.* **2015**, *30*, 311–329. [CrossRef]
13. Olivera, F. Extracting hydrologic information from spatial data for HMS modeling. *J. Hydrol. Eng.* **2001**, *6*, 524–530. [CrossRef]
14. Yang, D.; Gao, B.; Jiao, Y.; Lei, H.; Zhang, Y.; Yang, H.; Cong, Z. A distributed scheme developed for eco-hydrological modeling in the upper Heihe River. *Sci. China Earth Sci.* **2015**, *58*, 36–45. [CrossRef]
15. Garbrecht, J.; Ogden, F.L.; DeBarry, P.A.; Maidment, D.R. GIS and distributed watershed models. I: Data coverages and sources. *J. Hydrol. Eng.* **2001**, *6*, 506–514. [CrossRef]
16. Hornberger, G.M.; Boyer, E.W. Recent advances in watershed modelling. *Rev. Geophys.* **1995**, *33*, 949–957. [CrossRef]
17. Lindsay, J.B.; Francioni, A.; Cockburn, J.M. LiDAR DEM smoothing and the preservation of drainage features. *Remote Sens.* **2019**, *11*, 1926. [CrossRef]
18. Russell, P.P.; Gale, S.M.; Muñoz, B.; Dorney, J.R.; Rubino, M.J. A spatially explicit model for mapping headwater streams. *JAWRA J. Am. Water Resour. Assoc.* **2015**, *51*, 226–239. [CrossRef]
19. Avinash, K.; Deepika, B.; Jayappa, K.S. Basin geomorphology and drainage morphometry parameters used as indicators for groundwater prospect: Insight from geographical information system (GIS) technique. *J. Earth Sci.* **2014**, *25*, 1018–1032. [CrossRef]

20. Murphy, P.N.; Ogilvie, J.; Meng, F.R.; Arp, P. Stream network modelling using lidar and photogrammetric digital elevation models: A comparison and field verification. *Hydrol. Process.* **2008**, *22*, 1747–1754. [CrossRef]
21. Uuemaa, E.; Hughes, A.O.; Tanner, C.C. Identifying feasible locations for wetland creation or restoration in catchments by suitability modelling using light detection and ranging (LiDAR) digital elevation model (DEM). *Water* **2018**, *10*, 464. [CrossRef]
22. Hodgson, M.E.; Jensen, J.R.; Schmidt, L.; Schill, S.; Davis, B. An evaluation of LIDAR- and IFSAR- derived digital elevation models in leaf-on conditions with USGS Level 1 and Level 2 DEMs. *Remote Sens. Environ.* **2003**, *84*, 295–308. [CrossRef]
23. Wehr, A.; Lohr, U. Airborne laser scanning—An introduction and overview. *ISPRS J. Photogramm.* **1999**, *54*, 68–82. [CrossRef]
24. MacMillan, R.A.; Martin, T.C.; Earle, T.J.; McNabb, D.H. Automated analysis and classification of landforms using high-resolution digital elevation data: Applications and issues. *Can. J. Remote Sens.* **2003**, *29*, 592–606. [CrossRef]
25. USGS. Earth Explorer. Available online: https://earthexplorer.usgs.gov/ (accessed on 4 June 2021).
26. McMaster, K.J. Effects of digital elevation model resolution on derived stream network positions. *Water. Resour. Res.* **2002**, *38*, 131–139. [CrossRef]
27. Pirotti, F.; Tarolli, P. Suitability of LiDAR point density and derived landform curvature maps for channel network extraction. *Hydrol. Process.* **2010**, *24*, 1187–1197. [CrossRef]
28. MOURA, M.M.; Beskow, S.; Terra, F.S.; Mello, C.R.D.; CUNHA, Z.A.; Cassalho, F. Influence of different relief information sources on the geomorphological characterization of small watersheds. *Anais Acad. Bras. Ciênc.* **2021**, *93*, e20191317. [CrossRef]
29. Hopkinson, C.; Hayashi, M.; Peddle, D. Comparing alpine watershed attributes from LiDAR, Photogrammetric, and Contour-based Digital Elevation Models. *Hydrol. Process.* **2009**, *23*, 451–463. [CrossRef]